

International Journal of Pharmacology

ISSN 1811-7775





ISSN 1811-7775 DOI: 10.3923/ijp.2025.521.540



Research Article

Virtual Screening of Representative Natural Products Library for TGF-β-Mediated Liver Cirrhosis: An in silico and in vitro Multi-Target Study

^{1,2}Haytham Mohamedelfatih Mohamed Makki, ¹Ki-Hoon Park, ^{1,2,3}Youngbuhm Huh, ^{2,3,4}Ja-Eun Kim, ^{2,3,5}Ji Hyun Lee, ^{2,3,6}Hwajin Lee, ⁷Sunyoung Kim, ^{8,9}Hiroyuki Konishi, ¹⁰Na Young Jeong, ^{1,2,3}Junyang Jung and ¹¹Hyung-Joo Chung

Abstract

Background and Objective: Transforming Growth Factor Beta (TGF-β) significantly contributes to liver cirrhosis pathogenesis by promoting hepatic fibrosis. Drug discovery using molecular docking (MD) offers valuable insights into potential therapeutic candidates. This study investigated the early-stage discovery of potential natural drug candidates targeting the non-canonical TGF-β signaling pathway in liver cirrhosis pathogenesis. Materials and Methods: A virtual screening of the Korea Chemical Bank (KCB) natural compounds library was performed against key proteins, including TGF-β Receptor Type-1 (TGF-βR1), Focal Adhesion Kinase (FAK) and Phosphoinositide 3-Kinase (PI3K), using MD. Bioinformatics analysis identified additional targets such as Matrix Metallopeptidase 13 (MMP13) and explored pathway enrichments. The predicted Absorption, Distribution, Metabolism and Excretion (ADME) properties of promising compounds were evaluated. Experimental validation on HepG2 cells using RT-qPCR was conducted for the selected compounds. Results: TGF-BR1 binders from the KCB library exhibited higher binding affinities (-11.2 to -10.4 kcal/mol) than the reference inhibitor galunisertib (-10.0 kcal/mol). Bioinformatics identified MMP13 as a potential target for alcoholic liver cirrhosis, with enriched pathways related to cancer, p53 and PI3K-Akt signaling. Notably, dihydrosanguinarine (DHS) and eriocitrin showed promising inhibitory interactions with fibrogenic kinases. The ADMET analysis indicated DHS, trisindoline and α -Naphthoflavone (α -NF) as viable oral candidates. The RT-qPCR results highlighted luteolin's inhibitory effects, whereas diosmetin and α -NF upregulated target gene expressions. **Conclusion:** In silico findings underscore the potential of promising natural compounds for liver cirrhosis therapy. However, further in vitro and in vivo studies are needed to confirm their antifibrotic efficacy and therapeutic value.

Key words: Liver cirrhosis, TGF-β signaling pathway, molecular docking, natural compounds, bioinformatics, pharmacokinetics profile (ADMET)

Citation: Makki, H.M.M., K.H. Park, Y. Huh, J.E. Kim and J.H. Lee et al., 2025. Virtual screening of representative natural products library for TGF-β-mediated liver cirrhosis: An in silico and in vitro multi-target study. Int. J. Pharmacol., 21: 521-540.

Corresponding Author: Na Young Jeong, Department of Anatomy and Cell Biology, College of Medicine, Dong-A University, Seo-qu, Busan 49201, South Korea Junyang Jung, Department of Anatomy and Neurobiology, College of Medicine, Kyung Hee University, Dongdaemun-gu, Seoul, 02447, South Korea

Hyung-Joo Chung, Department of Anesthesiology and Pain Medicine, College of Medicine, Kosin University, Seo-gu, Busan 49267,

Copyright: © 2025 Haytham Mohamedelfatih Mohamed Makki et al. This is an open access article distributed under the terms of the creative commons attribution License, which permits unrestricted use, distribution and reproduction in any medium, provided the original author and source are credited.

Competing Interest: The authors have declared that no competing interest exists.

Data Availability: All relevant data are within the paper and its supporting information files.

¹Department of Anatomy and Neurobiology, College of Medicine, Kyung Hee University, Dongdaemun-gu, Seoul 02447, South Korea

²Department of Biomedical Science, Graduate School of Medicine, Kyung Hee University, Dongdaemun-gu, Seoul 02447, South Korea

³Department of Precision Medicine, College of Medicine, Kyung Hee University, Dongdaemun-gu, Seoul 02447, South Korea

⁴Department of Pharmacology, College of Medicine, Kyung Hee University, Dongdaemun-gu, Seoul 02447, South Korea

Department of Clinical Pharmacology and Therapeutics, College of Medicine, Kyung Hee University, Dongdaemun-gu, Seoul 02447, South Korea

Department of Biochemistry and Molecular Biology, College of Medicine, Kyung Hee University, Dongdaemun-gu, Seoul 02447, South Korea

⁷Department of Family Medicine, College of Medicine, Kyung Hee University Medical Center, Kyung Hee University, Dongdaemun-gu, Seoul 02447, South Korea

⁸Division of Neuroanatomy, Department of Neuroscience, Yamaguchi University, Graduate School of Medicine, 1-1-1 Minamikogushi, Ube,

Yamaguchi 755-8505, Japan

⁹Department of Functional Anatomy and Neuroscience, Nagoya University, Graduate School of Medicine, 65 Tsurumaicho, Showa-Ku, Nagoya, Aichi 466-8550, Japan

¹⁰Department of Anatomy and Cell Biology, College of Medicine, Dong-A University, Seo-gu, Busan 49201, South Korea

¹¹Department of Anesthesiology and Pain Medicine, College of Medicine, Kosin University, Seo-gu, Busan 49267, South Korea

INTRODUCTION

Liver cirrhosis (LC) is a chronic liver disease that results from various etiologies, including viral hepatitis, alcohol abuse and non-alcoholic fatty liver disease. It is associated with significant morbidity and mortality worldwide. Often, liver cirrhotic patients end with the emergence of Hepatocellular Carcinoma (HCC)^{1,2}.

One of the key molecular pathways involved in the pathogenesis of liver cirrhosis is the Transforming Growth Factor Beta (TGF-β) signaling pathway. The TGF-β pathway plays a crucial role in the regulation of cell growth, differentiation and tissue homeostasis. TGF-β ligands bind to TGF-B receptors, leading to the activation of downstream signaling cascades, including the canonical Smad-dependent pathway and non-Smad signaling pathways such as MAPK and PI3K/Akt. Dysregulation of the TGF-β pathway has been implicated in the development and progression of liver cirrhosis^{3,4}. The TGF-β plays a pivotal role in hepatic fibrosis, the hallmark of liver cirrhosis. It promotes the activation of Hepatic Stellate Cells (HSCs) into myofibroblasts, which are responsible for excessive production and deposition of Extracellular Matrix (ECM) components, such as collagen. The TGF-β induces the expression of ECM proteins and inhibits their degradation, leading to ECM accumulation and fibrotic scar formation^{5,6}.

Given the significant role of the TGF- β in LC, targeting this pathway has emerged as a potential therapeutic strategy. Several preclinical and clinical studies have explored the efficacy of TGF- β pathway inhibitors, such as TGF- β receptor type-1 (TGF- β R1) inhibitors: galunisertib and vactosertib^{7,8}.

In silico is computational analysis and simulation performed on a computer, using algorithms, mathematical models and molecular dynamics to study biological systems without time-consuming experiments. In drug discovery, in silico methods are important for identifying potential drug candidates through virtual screening of chemical libraries against target proteins, enabling rapid identification of compounds with high binding affinity, specificity and low toxicity. Molecular Docking (MD) is a specific in silico technique used to predict binding mode and affinity between a small molecule and a protein receptor. This information is useful for understanding drug mechanisms, optimizing lead compounds and designing new molecules with improved pharmacological properties⁹⁻¹¹.

Natural compounds have long been a valuable source of therapeutic candidates in drug discovery and development.

Many of these compounds have shown promising biological activities and therapeutic potential in treating various diseases. It's important to note that while natural compounds show promise, their development into the rapeutic drugs often involves further research, clinical trials and safety assessments. Additionally, the effectiveness of these compounds may vary depending on factors such as dosage, bioavailability and interaction with other medications¹². Drugs with a single target might be ineffective in preventing or curing diseases that induce pathogenesis via multiple target pathways¹³. Recently, several research studies were conducted by virtual screening of natural compounds against multiple targets in LC/HCC¹⁴⁻¹⁷. Therefore, this multi-target approach study aimed to investigate promising candidates from the KCB representative natural compounds library targeting TGF-BR1, FAK and PI3K through the MD technique. Another approach was to predict and identify potential protein targets related to LC through bioinformatics...

MATERIALS AND METHODS

Study area: This study was conducted for 9 months (April to December, 2023) at the Department of Anatomy and Neurobiology, College of Medicine, Kyung Hee University (Seoul Campus).

Software: Discovery Studio Client (BIOVIA, Dassault Systèmes, v21.1.0, San Diego, 2021), AutoDockTools(v1.5.7)¹⁸, OpenBabelGUI (v2.4.1)¹⁹, AutoDock Vina²⁰ and Padre, the Perl-integrated Development Environment (IDE) were used in a Samsung notebook with specifications: Intel(R) Celeron(R) 6305 @1.80GHz, Windows 10 Education, 64-bit OS and 12.0 GB RAM.

Receptor and ligand preparations: The three-dimensional (3D) structures of the target proteins TGFβR1, FAK and PI3K with PDB IDs: 5E8S²¹, 3BZ3²² and 5T23²³, respectively (Table S1), were downloaded in PDB file format from the Research Collaboratory for Structural Bioinformatics (RCSB) database²⁴. Using the Discovery Studio Client software, each receptor was modified by deleting water molecules, obtaining XYZ values of the active binding sites for docking based on the original ligand in the crystal complex, followed by deleting the contaminant ligands. Then, the free-ligand receptor was opened in the AutoDockTools software for adding polar hydrogens and Kollman charges and finally saved in PDBQT format.

A total of 1278 ligands in PDB file format were obtained from the representative natural compounds library in KCB and then converted to 3D structures in PDBQT format using OpenBabelGUI software. Galunisertib (CID: 10090485) and vactosertib (CID: 54766013) were downloaded from PubChem in SDF format and then converted to AutoDock Structure File (PDBOT) format.

Molecular docking (MD): After collecting all required PDBQT files in one folder, the docking of up to 100 ligands into each targeted receptor per session was executed in AutoDock Vina and Padre, the Perl IDE software using the command prompt "perl Vina_windows.pl".

Prediction and identification of potential targets related to alcoholic liver cirrhosis (ALC) and KCB natural compounds: The genes associated with ALC were obtained from DisGeNET²⁵. However, the promising targets related to the best TGFβR1 binders among KCB natural compounds were predicted using SwissTargetPrediction²⁶. Overlapped genes were identified using an online VENNY (v2.1.0) diagram tool.

Gene ontology (GO) and Kyoto encyclopedia of genes and genomes (KEGG) pathway enrichment analysis: The identified overlapped genes were uploaded into the Database for Annotation, Visualization and Integrated Discovery (DAVID)²⁷ bioinformatics database for the gene functional annotation, including GO and KEGG analyses.

Protein-protein interaction (PPI) network analysis: The overlapped gene targets were uploaded into the STRING database²⁸ (v12.0), which provides evaluation and integration of both physical and functional protein-protein interactions. Then, the PPI information was visualized with Cytoscape²⁹ (v3.10.0), which is an open-source software platform that pathways while also combining annotations, gene expression profiles and other state data.

In silico **prediction of the ADMET profile and bioactivity score:** The SMILES structures of the top ten KCB hit compounds and the reference inhibitors were uploaded to online web tools, ADMETlab³⁰ (v2.0) and SwissADME³¹. These web tools provide estimations for the pharmacokinetic profile (absorption, distribution, metabolism, excretion and toxicity, ADMET) in addition to the physicochemical and oral

druggable properties of the small molecules. The SDF files of small molecules were uploaded to Molinspiration cheminformatics (Molinspiration Cheminformatics free web services, Slovensky Grob, Slovakia), which is a free web tool used to predict bioactivity scores for important drug targets such as kinases and nuclear receptors.

Experimental validation using cell viability assay and RT-qPCR: To validate the protein-ligand affinities the effects of three compounds, Luteolin (Cat. No. 2874, Tocris Bioscience), Diosmetin (Cat. No. D7321, Sigma-Aldrich) and Alpha-naphthoflavone (α-NF; Cat. No. N5757, Sigma-Aldrich) were tested on human hepatoma (HepG2) cells, which were obtained from the Korean cell line bank (KCLB, Cat. No. 88065, Seoul, South Korea) and maintained at 37°C with 5% CO₂ in minimum essential medium (MEM, Cat. No. 11095080, Gibco™, Billings, Montana, USA) supplemented with 25 mM HEPES, 25 mM NaHCO₃ and 10% FBS. Drugs were diluted in MEM to the required working concentrations and then incubated with 3000 cells/well in a 96-well plate for 48 hrs to detect cell viability using MTS assay (CellTiter 96® AQueous One Solution Cell Proliferation Assay, Cat. No. G3581, Promega) according to the manufacturer's protocol. Moreover, examined the mRNA expressions of the target proteins using RT-qPCR as previously described by Park et al.32. Briefly, cells were cultured in a 6-well plate for 24 hrs and then the media was replaced with a drug-containing media for another 24 hrs. used Trizol® Reagent (Cat. No. 15596-026, Invitrogen, Carlsbad, California, USA) for total RNA extraction from cells of each group. To make cDNA from RNA templates, used oligo-dT primers and the Superscript III First-Strand kit (Cat. No. 18080-044, Invitrogen). Finally, the RT-qPCR reaction on the Takara Thermal Cycler Dice Real Time System Lite (Takara Bio CO., Otsu, Japan) with 10 ng of cDNA was conducted, 4 pmoles of each gene-specific primer and TB Green Premix Ex Taq (Cat. No. RR420A, Takara Bio Co., Otsu, Japan) following the manufacturer's protocol of 20 μL reaction. The sequences of forward and reverse primers were

Statistical analysis: The data from *in vitro* analysis were analyzed using GraphPad Prism 8.0.2 software (GraphPad Software, Inc., CA, USA). Two-tailed unpaired Student's t-test or one-way ANOVA analyses followed by Dunnett's *post hoc* tests for multiple comparisons were carried out. Data were expressed as Mean±SEM. Significant differences were symbolled with *p<0.05.

listed in Table S2.

RESULTS AND DISCUSSION

Visualization of 3D structural data of the targeted proteins:

The three-dimensional (3D) structural models of TGFBR1 (Fig. 1a), FAK (Fig. 1b) and PI3K (Fig. 1c) proteins were meticulously visualized employing the Discovery Studio Client software. This tool enabled an in-depth structural analysis and presentation of these proteins. Among KCB's natural compounds, a specific selection process was undertaken, focusing on identifying the ten ligands exhibiting the lowest binding affinity values, expressed in kcal/mol, towards the TGFBR1 protein. These selected ligands were then subjected to a detailed two-dimensional (2D) visualization process to highlight their structural features and interactions. The 2D structures of the reference TGFBR1 inhibitors, galunisertib (Fig. 1d) and vactosertib (Fig. 1e) were represented with the top-ranked TGFBR1 binders, which are Dihydrosanguinarine (Fig. 1f), Quercetin 7-O-glucoside (Fig. 1g), Eriocitrin (Fig. 1h), Diosmetin-7-O-rutinoside (Fig. 1i), Myricetin (Fig. 1j), Trisindoline (Fig. 1k), Luteolin-8-C-glucoside (Fig. 1l), Luteolin 7-galactoside (Fig. 1m), 3-Oxolup-20(29)-en-28-oic acid (Fig. 1n) and Alpha-naphthoflavone (Fig. 1o).

MD with AutoDock Vina: Docking results between the macromolecule (protein) and the small molecules (ligands) were presented in terms of binding affinity, measured in kcal/mol, in correlation with RMSD (Root Mean Square Deviation) values. Binding affinity indicates the strength of the interaction between the protein and ligand, while RMSD values measure the positional deviation of docked ligand poses from a reference pose. In docking studies, the method's success is often defined by achieving RMSD values of less than 2.0 angstroms (Å)³³, as this indicates high structural similarity and stability. The RMSD values falling within the range of 3.0>RMSD>2.0 Å are still acceptable³⁴. From the ten output docking poses generated for each ligand, the pose that exhibited the lowest binding affinity value was selected, as it was deemed to represent the most energetically favorable and thus likely the most accurate binding mode.

MD of KCB natural compounds with the target protein kinases: The docking analysis of TGFBR1 showed binding affinity values that varied significantly, ranging from -11.2 to -2.2 kcal/mol (Fig. 2a). For the FAK target, the binding affinity analysis produced values that ranged from -11.4 to -3.9 kcal/mol, in Fig. 2b. This range suggests that the ligands have varying degrees of binding strength with FAK. In Fig. 2c, the binding affinity values for the kinase

protein PI3K are depicted, with a range spanning from -10.6 to -3.8 kcal/mol. This analysis reveals that some ligands show strong binding potential with PI3K, as evidenced by their lower kcal/mol scores. These results highlight the promising binding potential of KCB natural compounds, which outperformed the reference inhibitors in terms of binding affinity, suggesting their potential as effective alternatives to the current standard inhibitors in targeting TGFBR1, FAK and PI3K.

Specifically, the heatmap illustrated in Fig. 2d and Table S3 highlights the top ten ligands that exhibited the highest binding affinity to TGFBR1, FAK and PI3K, comparing these values with those of known TGFBR1 inhibitors, galunisertib and vactosertib. With TGFBR1, these reference inhibitors presented binding affinity values of -10 and -10.6 kcal/mol, respectively. However, when interacted with FAK, galunisertib and vactosertib demonstrated binding affinity values of -10.7 and -9.7 kcal/mol, respectively. Notably, two natural compounds, eriocitrin (-10.5 kcal/mol) and alpha-naphthoflavone (-10.1 kcal/mol), exhibited binding scores that were lower than those of the reference inhibitors galunisertib (-9.4 kcal/mol) and vactosertib (-9.3 kcal/mol). These reference values provide a benchmark for evaluating the effectiveness of other ligands in binding to TGFBR1, FAK and PI3K and indicate that some tested ligands may offer stronger interactions with these kinases than the reference inhibitors.

Additionally, the RMSD results provided insights into the docking stability of these ligands. The analyzed ligands demonstrated optimal docking poses, particularly when the RMSD values were at or below 2.0 Å, indicating a close match to the reference inhibitor, vactosertib. This finding suggests that these ligands are highly compatible in terms of binding conformation. However, some ligands showed acceptable docking poses, with RMSD values falling within the range of 3.0 >RMSD >2.0 Å, about the reference inhibitor galunisertib, as illustrated in Fig. 2e. These values reflect a less precise but still acceptable alignment in binding pose with the galunisertib reference structure.

Visualization of the receptor-ligand interactions: Biovia Discovery Studio 2021 was used to visualize the two-dimensional (2D) interactions between the TGFβR1 and the KCB natural compounds in comparison with the canonical TGFβR1 inhibitors: galunisertib and vactosertib. Figure 3 represented the interacted amino acid residues ofTGFβR1 through bonds of conventional hydrogen, pi-sigma and alkyl/pi-alkyl. Particularly, TGFβR1 could be interacted through

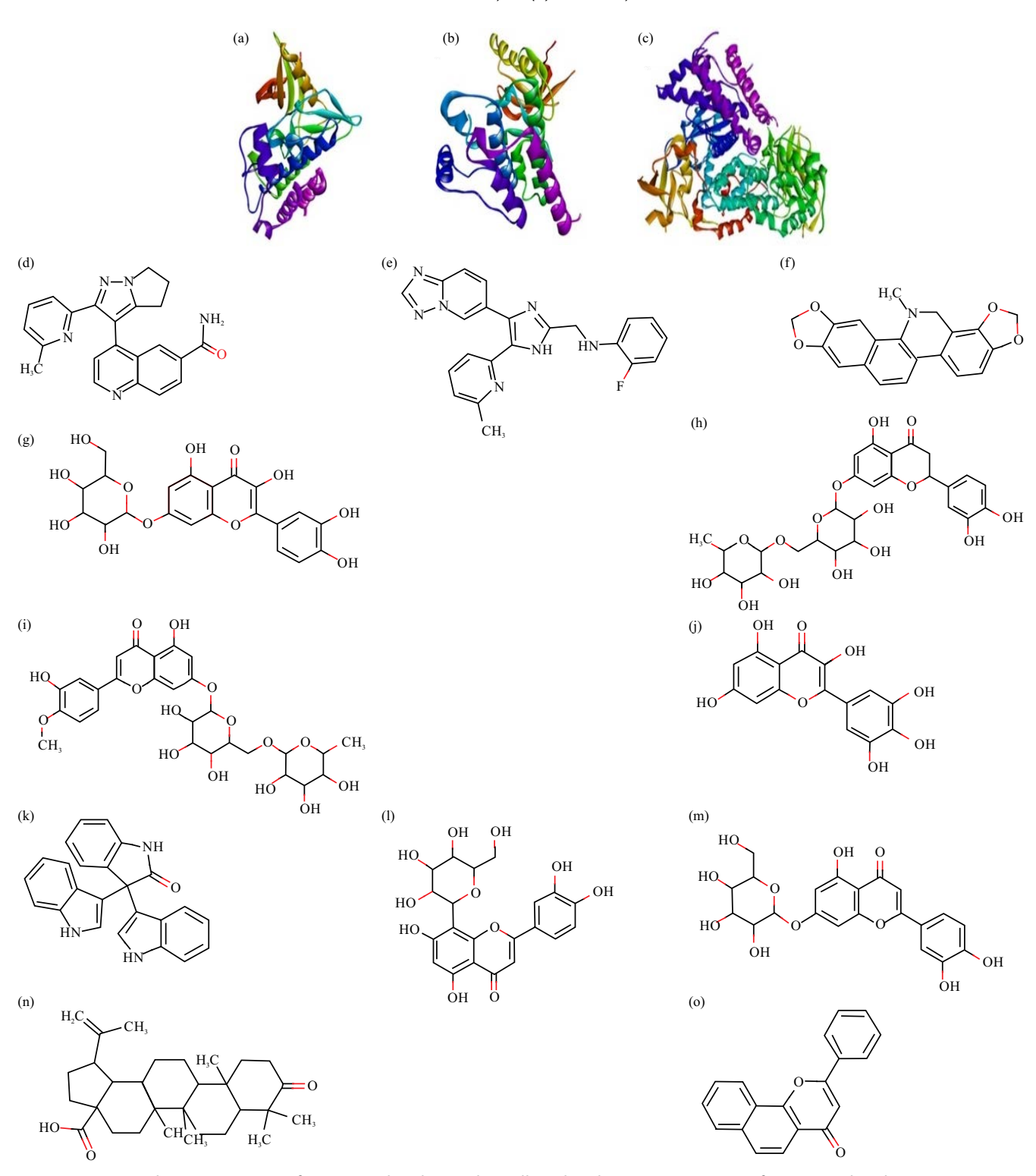


Fig. 1(a-o): 3D and 2D structures of macromolecules and small molecules, 3D structures of macromolecules (proteins) are: (a) TGFBR1 (PDB: 5E8S), (b) FAK (PDB: 3BZ3) and (c) PI3K (PDB: 5T23), The 2D structures of small molecules (ligands) are: (d) Galunisertib: Known TGFBR1 inhibitor with antifibrotic properties, (e) Vactosertib: Another TGFBR1 inhibitor targeting fibrosis mechanisms, The top 10 of KCB natural compounds having the best docking scores with TGFBR1, including: (f) Dihydrosanguinarine, (g) Quercetin 7-O-glucoside, (h) Eriocitrin, (i) Diosmetin-7-O-rutinoside, (j) Myricetin, (k) Trisindoline, (l) Luteolin-8-C-glucoside, (m) Luteolin 7-galactoside, (n) 3-Oxolup-20(29)-en-28-oic acid, (o) Alpha-naphthoflavone

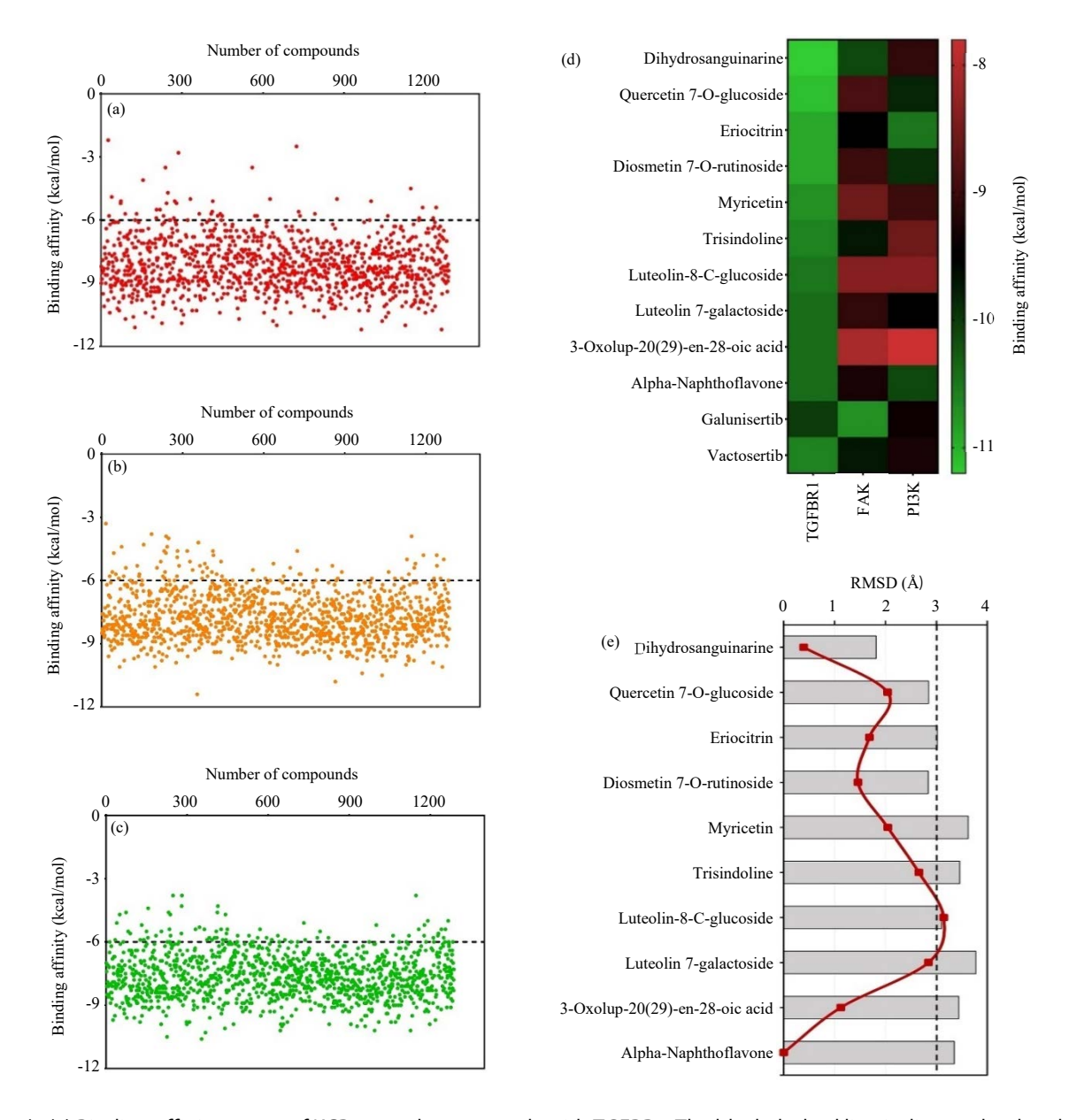


Fig. 2(a-e): (a) Binding affinity scores of KCB natural compounds with TGFBR1. The black dashed line indicates the threshold for strong binding (≤-6.0 kcal/mol), (b) Binding affinity scores of KCB natural compounds with FAK. The black dashed line shows the strong binding threshold (≤-6.0 kcal/mol), (c) Binding affinity scores of KCB natural compounds with PI3K. The black dashed line marks the favorable binding threshold (≤-6.0 kcal/mol), (d) Heatmap of the best binding scores of KCB compounds compared with reference TGFBR1 inhibitors, Galunisertib and Vactosertib and (e) RMSD values of docked ligands normalized to reference inhibitors. Galunisertib is shown as grey columns, Vactosertib as a dark red line. The black dashed line represents the acceptable deviation threshold (<3 Å)

the conventional hydrogen binding to the amino acids: Isoleucine (ILE211), glycine (GLY214) lysine (LYS232, LYS337), glutamic acid (GLU245), tyrosine (TYR249), leucine (LEU278), serine (SER280, SER287), aspartic acid (ASP281, ASP290, ASP351), histidine (HIS283) and asparagine (ASN338) (Fig. 3). The results revealed that FAK could be inhibited by

dihydrosanguinarine (Fig. 4a) and galunisertib (Fig. 4b) at the binding sites: ASP564, LEU567, LEU553, valine (VAL436), alanine (ALA452), VAL484 and methionine (MET499). However, PI3K interacted through conventional hydrogen bonds with eriocitrin (Fig. 4c) at LYS833, VAL882, ASP950 and ASP964 but with vactosertib (Fig. 4d) at threonine (THR887).

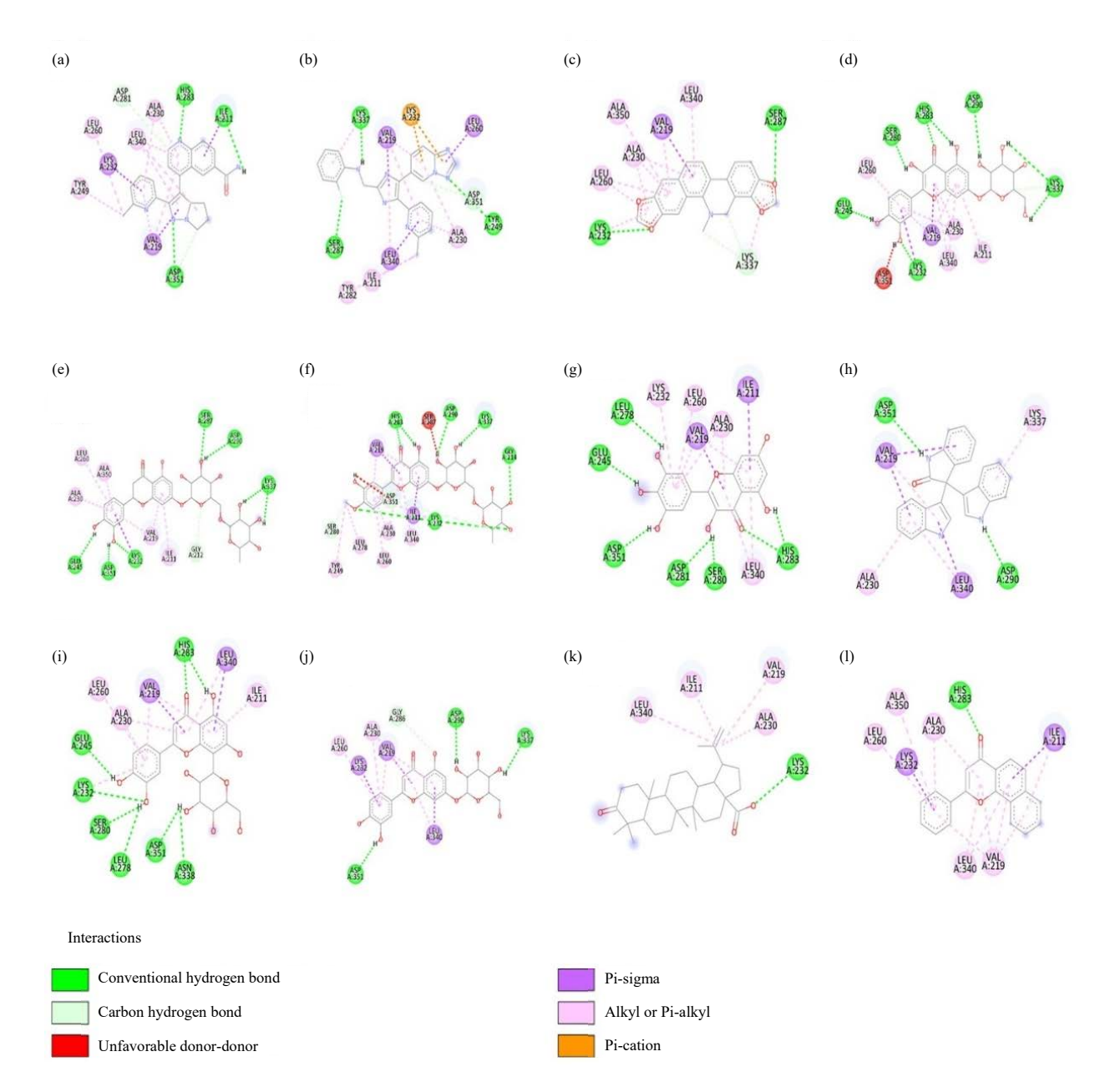


Fig. 3(a-i): 2D interaction maps of TGFBR1 with reference inhibitors and KCB natural compounds, (a) Galunisertib with TGFBR1, showing hydrogen bonds and hydrophobic interactions with key amino acid residues, (b) Vactosertib with TGFBR1, highlighting stabilizing interactions with specific residues, (c) DHS with TGFBR1, indicating favorable contacts contributing to ligand affinity, (d) Quercetin 7-O-glucoside with TGFBR1, displaying bonding patterns that support stable binding, (e) Eriocitrin with TGFBR1, identifying crucial amino acid contacts and bonding types, (f) Diosmetin-7-O-rutinoside with TGFBR1, showing hydrogen bonding and hydrophobic forces, (g) Myricetin with TGFBR1, with labeled residues involved in stabilizing the ligand, (h) Trisindoline's 2D interaction with TGFBR1, emphasizing contacts that may enhance binding strength, (i) Luteolin-8-C-glucoside interaction map, demonstrating stabilizing bonds with TGFBR1 residues, (j) Luteolin 7-galactoside with TGFBR1, outlining key residue engagements, (k) OOA with TGFBR1, revealing hydrogen bonds and hydrophobic interactions and (l) Alpha-NF with TGFBR1, showing molecular forces contributing to ligand stabilization

These interaction diagrams collectively provide molecular insights into how each compound engages with the TGFBR1 binding pocket, comparing natural compounds with reference inhibitors

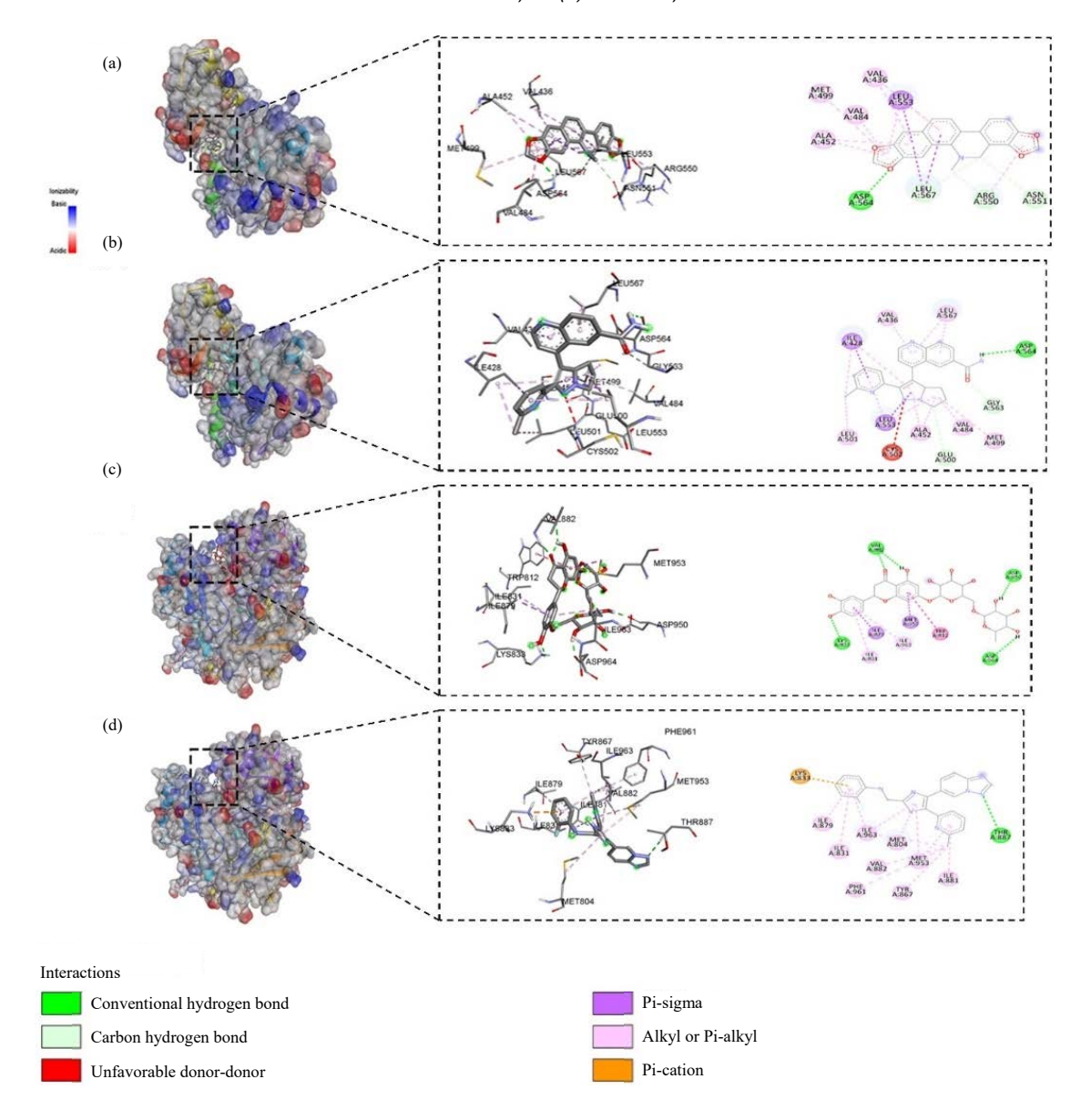


Fig. 4(a-e): Molecular docking visualization of interactions with FAK and Pl3K, (a) 3D docking visualization of DHS with FAK, highlighting its spatial orientation and interaction within the active site, (b) 3D docking pose of Galunisertib with FAK, showing its binding alignment and key contact regions, (c) 3D interaction of Eriocitrin with Pl3K in ionized form, illustrating the molecular docking conformation and critical binding interactions, (d) 3D docking model of Vactosertib with Pl3K, displaying spatial positioning and interaction points within the binding pocket and (e) Combined 3D and 2D representations of docking interactions for the ligands, detailing hydrogen bonds, hydrophobic contacts and interacting amino acid residues involved in stabilizing ligand binding with FAK and Pl3K

Bioinformatics analysis: A total of 126 gene targets associated with ALC were obtained from DisGeNET. However, a total of a hundred gene targets per each KCB natural compounds were predicted using SwissTargetPrediction. Then, a total of 17 overlapped genes were identified including Matrix Metallopeptidase 2 (MMP2), Cytochrome P450 Family 1 Subfamily A Member 1 (CYP1A1), Arginase 1 (ARG1), Vitamin D Receptor (VDR), Angiotensin Converting

Enzyme (ACE), Peroxisome Proliferator Activated Receptor Gamma (PPARG), MDM2 Proto-Oncogene (MDM2), BCL2 apoptosis regulator (BCL2), Tumor Protein p53 (TP53), Tumor Necrosis Factor (TNF), Matrix Metallopeptidase 13 (MMP13), myeloperoxidase (MPO), aldehyde dehydrogenase 2 family member (ALDH2), interleukin 2 (IL2), nitric oxide synthase 2 (NOS2), aldo-keto reductase family 1 member A1 (AKR1A1) and albumin (ALB) (Fig. 5a).

The PPI network analysis revealed that the network consisted of 17 nodes and 62 edges. Moreover, the interaction enrichment p-value was calculated as 1.89e-15, indicating that these proteins have more interactions with one another than would be predicted and at the very least, they were loosely physiologically linked (Fig. 5b).

The GO of cell component (GO_CC) revealed that the identified genes were enriched in the extracellular space, nucleus and mitochondrion (Fig. 5c). Related to biological processes (GO_BP), the target genes were enriched in response to xenobiotics-induced oxidative stress, inducing apoptosis or inflammation and ECM organization (Fig. 5d). In terms of molecular functions (GO_MF), the target genes were enriched in enzyme binding, metalloendopeptidase (MEP) activity, p53 binding and chaperone binding (Fig. 5e). Finally, the KEGG pathway analysis showed off that the promising gene targets were significantly enriched in cancer-inducing pathways, p53 or PI3K-Akt signaling pathways (Fig. 5f).

Another virtual screening was executed using the predicted potential target MMP13 with PDB ID: 4A7B³⁵ and the best TGFβR1 binders among the KCB hit compounds in addition to the reference ligands. The results revealed that the docked ligands to MMP13 have lower affinity scores in chain B than chain A as shown in Table S4.

ADMET profile predictions: The results of oral bioavailability were assessed using SwissADME according to six physicochemical properties: lipophilicity, size, polarity, water solubility, flexibility and saturation. The results of the bioavailability radar demonstrated that DHS and trisindoline were closely similar to galunisertib and vactosertib (Fig. 6). Regarding the pharmacokinetic profile, the results of

ADMETIab 2.0 revealed that DHS and alpha-Naphthoflavone (α-NF) had optimal absorption parameters (Caco-2 cell permeability >-5.15 log unit and human intestinal absorption (HIA)³ 30%) as compared to reference compounds (Fig. 7 and Fig. 8a). The metabolism results represented DHS and trisindoline as potential inhibitors of the cytochrome P450 (CYP) isoenzymes (Fig. 7). Moreover, the distribution profile represented four compounds with plasma protein binding (PPB) percentage out of the optimal range, however, 3-Oxolup-20(29)-en-28-oic acid (OOA) showed off higher blood-brain barrier (BBB) penetration score (Fig. 8b). The excretion parameters noted that DHSG had the highest clearance with a shorter half-life time (T_{1/2}) than vactosertib (Fig. 8c). In toxicity prediction, the results exhibited that KCB hit compounds had no cardiotoxic (hERG) nor human hepatotoxic (H-HT) effects as compared to galunisertib and vactosertib, however, OOA revealed non-mutagenic (Ames) and non-carcinogenic effects (Fig. 7).

Furthermore, the oral drug-likeness assessment was obtained from SwissADME according to five different rule-based filters, which are used by major pharmaceutical companies: Lipinski (Pfizer)³⁶, Ghose (Amgen)³⁷, Veber (GSK)³⁸, Egan (Pharmacia)³⁹ and Muegge (Bayer)⁴⁰ filters. As shown in Fig. 8d, DHS, trisindoline and α -NF exhibited no violations in the drug-likeness filters as compared to galunisertib and vactosertib.

The predicted bioactivity scores in Molinspiration cheminformatics revealed that DHS and OOA had higher scores as G Protein-Coupled Receptor (GPCR) ligands in compare to galunisertib. Moreover, DHS and myricetin could be bioactive as kinase inhibitors. As a nuclear receptor ligand, OOA exhibited the best score as compared to the reference inhibitors (Table 1).

Table 1: Predicted bioactivity scores in Molinspiration cheminformatics

			Ion channel		Nuclear	Protease	
Compound No. Small molecule GPCR li		GPCR ligand	modulator	Kinase inhibitor	receptor ligand	inhibitor	Enzyme inhibitor
1252	Dihydrosanguinarine	0.19	0.09	0.23	0.16	0.00	0.16
125	Quercetin 7-O-glucoside	0.04	-0.10	0.15	0.23	-0.06	0.42
225	Eriocitrin	0.06	-0.47	-0.28	-0.08	0.05	0.16
298	Diosmetin-7-O-rutinoside	-0.05	-0.53	-0.13	-0.23	-0.06	0.09
90	Myricetin	-0.06	-0.18	0.28	0.32	-0.20	0.30
119	Trisindoline	0.05	-0.07	0.01	-0.17	-0.11	-0.07
304	Luteolin-8-C-glucoside	0.12	-0.14	0.20	0.20	0.01	0.45
33	Luteolin 7-galactoside	0.09	-0.02	0.15	0.27	-0.01	0.42
164	3-Oxolup-20(29)-en-28-oic acid	0.21	-0.06	-0.69	0.88	0.04	0.47
438	Alpha-naphthoflavone	-0.09	-0.31	0.20	0.12	-0.36	0.12
-	Galunisertib	0.12	-0.13	1.13	0.59	0.06	0.25
-	Vactosertib	0.27	-0.01	1.03	-0.45	0.09	0.30

More positive the value of the score, the greater the chance that the small molecule could be bioactive

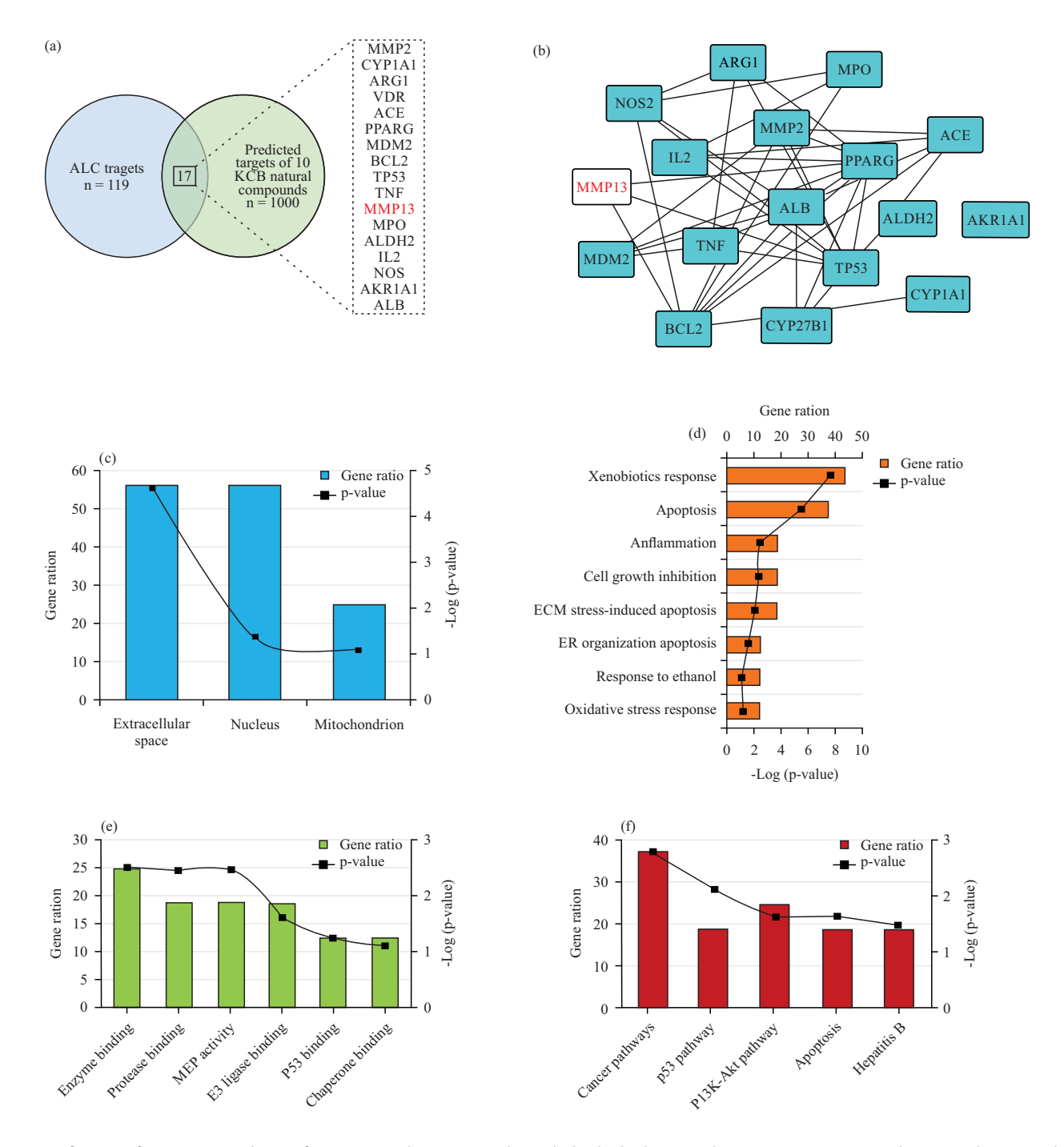


Fig. 5(a-f): Bioinformatics analysis of KCB natural compounds and alcoholic liver cirrhosis (ALC), (a) Venn diagram showing the overlap between KCB hit compound targets and ALC-related targets, identifying shared molecular pathways potentially involved in liver cirrhosis, (b) STRING PPI network illustrating predicted protein-protein interactions among the common targets, highlighting their connectivity and functional relationships, (c) Gene Ontology (GO) enrichment analysis-cellular component: Classification of targets based on their cellular localization and structural context, (d) GO enrichment analysis-biological process: Categorization of targets by their roles in biological activities relevant to ALC, (e) GO enrichment analysis-molecular function: Analysis of functional roles played by target proteins at the molecular level and (f) KEGG pathway enrichment analysis identifying key signaling pathways, such as p53 and PI3K-Akt, associated with the predicted targets, shedding light on possible mechanisms in liver cirrhosis pathogenesis

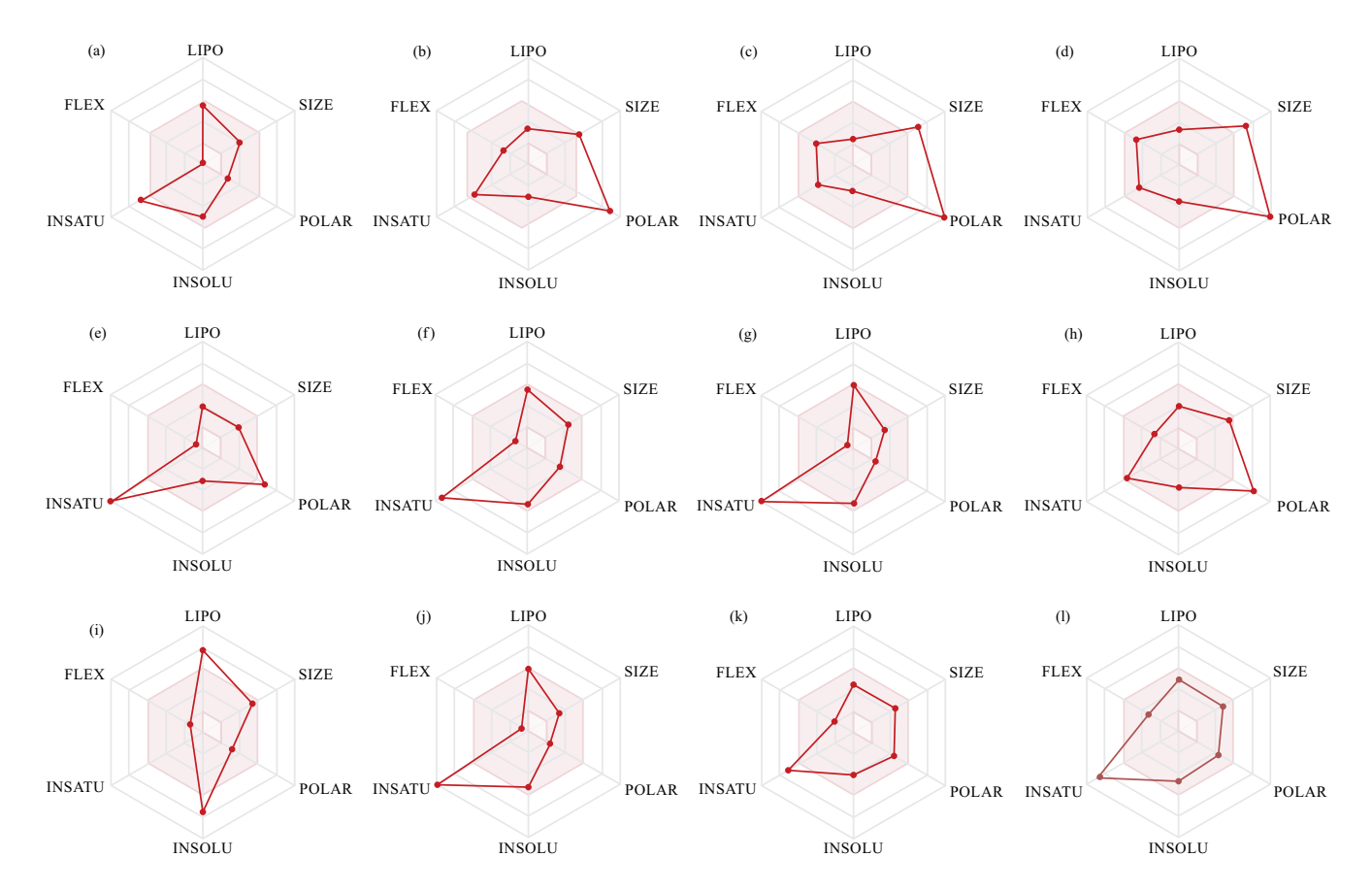


Fig. 6(a-I): Physicochemical properties of KCB hit compounds, (a) DHS, (b) Quercetin 7-O-glucoside, (c) Eriocitrin, (d) Diosmetin-7-O-rutinoside, (e) Myricetin, (f) Trisindoline, (g) Luteolin-8-C-glucoside, (h) Luteolin 7-galactoside, (i) OOA, (j) α-NF, (k) Galunisertib and (l) Vactosertib

The pink area represents the optimal range for each property: lipophilicity (LIPO): XLOGP3 between -0.7 and +5.0, size: MW between 150 and 500 g/mol, polarity (POLAR): TPSA between 20 and 130 Å2, solubility (INSOLU): log S not higher than 6, saturation (INSATU): Fraction of carbons in the sp3 hybridization not less than 0.25 and flexibility (FLEX): No more than 9 rotatable bonds

Experimental validation of the virtual screening results: The

MD findings revealed that both luteolin (Fig. 9a) and diosmetin (Fig. 9b) had good multitarget binding affinities (Fig. 9c), which were found to interact with HIS283 and SER280 by conventional hydrogen bonds (Fig. 9d-e). Therefore, these findings were experimentally validated by investigating the effects of three flavonoid compounds: Luteolin, diosmetin and α-NF on HepG2 cells using cell viability and RT-qPCR analyses. In comparison with the untreated control cells, luteolin and diosmetin inhibited but α -NF induced the cell proliferation dose-dependently; luteolin and diosmetin exhibited calculated Half-Maximal Inhibitory Concentration (IC₅₀) values of 35 and 70 μ M. However, α-NF revealed a calculated half-maximal effective concentration (EC₅₀) at 867 µM (Fig. 10a-b). However, RT-qPCR analysis revealed that luteolin inhibited the mRNA expressions of the targeted proteins at the higher concentrations (Fig. 10c) but both diosmetin and α -NF upregulated the target proteins in a dose-dependent manner (Fig. 10d-e).

Cirrhosis is the end stage of any chronic liver disease, regardless of the etiology. It is characterized by liver parenchyma deformation, fibrous septae, nodules and blood flow changes. Clinically, LC starts as an asymptomatic compensated phase and then proceeds to a decompensated phase, causing complications like ascites, jaundice, portal hypertension and hepatic encephalopathy^{41,42}. Treatment of LC depends on the etiology removal such as abstinence from alcohol or using antivirals. However, no direct antifibrotic medicine is currently available, making it critically needed. Direct antifibrotic treatment seeks to reduce scar formation or hasten the healing process. Therefore, inhibition of the TGF- β signaling pathway is considered a potential target to create effective antifibrotic medicines^{43,45}.

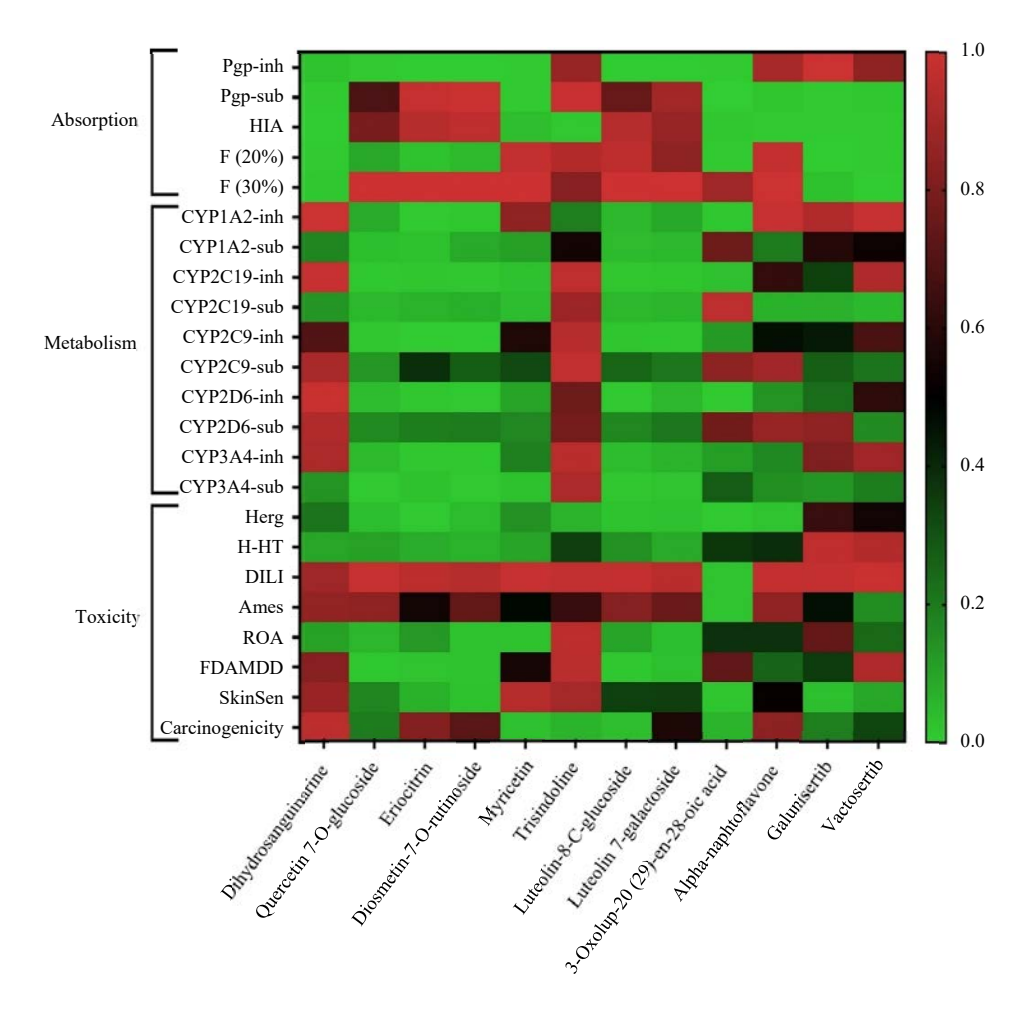


Fig. 7: In silico pharmacokinetics (PK) profile evaluation of KCB hit compounds

Heatmap of absorption, metabolism and toxicity; Category 0: non-inhibitor, non-substrate, or non-toxic; Category 1: Inhibitor, substrate or toxic. The output value is the probability of being inhibitor, substrate, or toxic, within the range of 0 to 1. HIA; Category 0: HIA >30%; Category 1: HIA <30%. Toxicity: Category 0: Negative (-); Category 1: Positive (+). The output value is the probability of being toxic within the range of 0 to 1. Empirical decision: 0-0.3: Excellent (green); 0.3-0.7: Medium (black) and 0.7-1.0: Poor (red)

This study, performed a virtual screening of the KCB natural compounds library in order to screen promising compounds with potential inhibitory effects on TGF-mediated LC. In MD, the binding affinity score explains the interaction stability and the small molecule's potency to either induce or inhibit the macromolecule as indicated with the lowest value of binding affinity^{46,47}, preferably \leq -6 kcal/mol⁴⁸. The results revealed potent TGF β R1 binders with lower binding scores compared to the reference inhibitors (Fig. 2). Moreover, it has been reported that MD with AutoDock Vina predicted the inhibitory interaction of 5E8S, which was suppressed via hydrogen bonds with SER288, LYS337 and ASP351⁴⁹, these findings correlated with current results suggesting that these residues are essential for TGF β R1 interactions (Fig. 3).

Both Focal Adhesion Kinase (FAK) and Phosphoinositide 3-Kinase (PI3K) play significant roles in the pathogenesis of

liver cirrhosis. Their activation contributes to HSCs activation, ECM production and cell survival, ultimately leading to the development and progression of liver fibrosis and cirrhosis. Targeting FAK and PI3K signaling pathways may offer potential therapeutic strategies to mitigate liver fibrosis and its associated complications^{50,51}. Current results showed off hit compounds with lower affinity scores than the reference compounds and thus indicating potential inhibitory effects against FAK and PI3K (Fig. 2). Moreover, current results in Fig. 4 exhibited the same binding sites of interactions with FAK but less similarity with PI3K as reported by other studies in the literature⁵²⁻⁵⁴. Thus, the affinity scores with visualization of the interactions could provide clear evidence that these macromolecules could be inhibited through binding to the aforementioned amino acids.

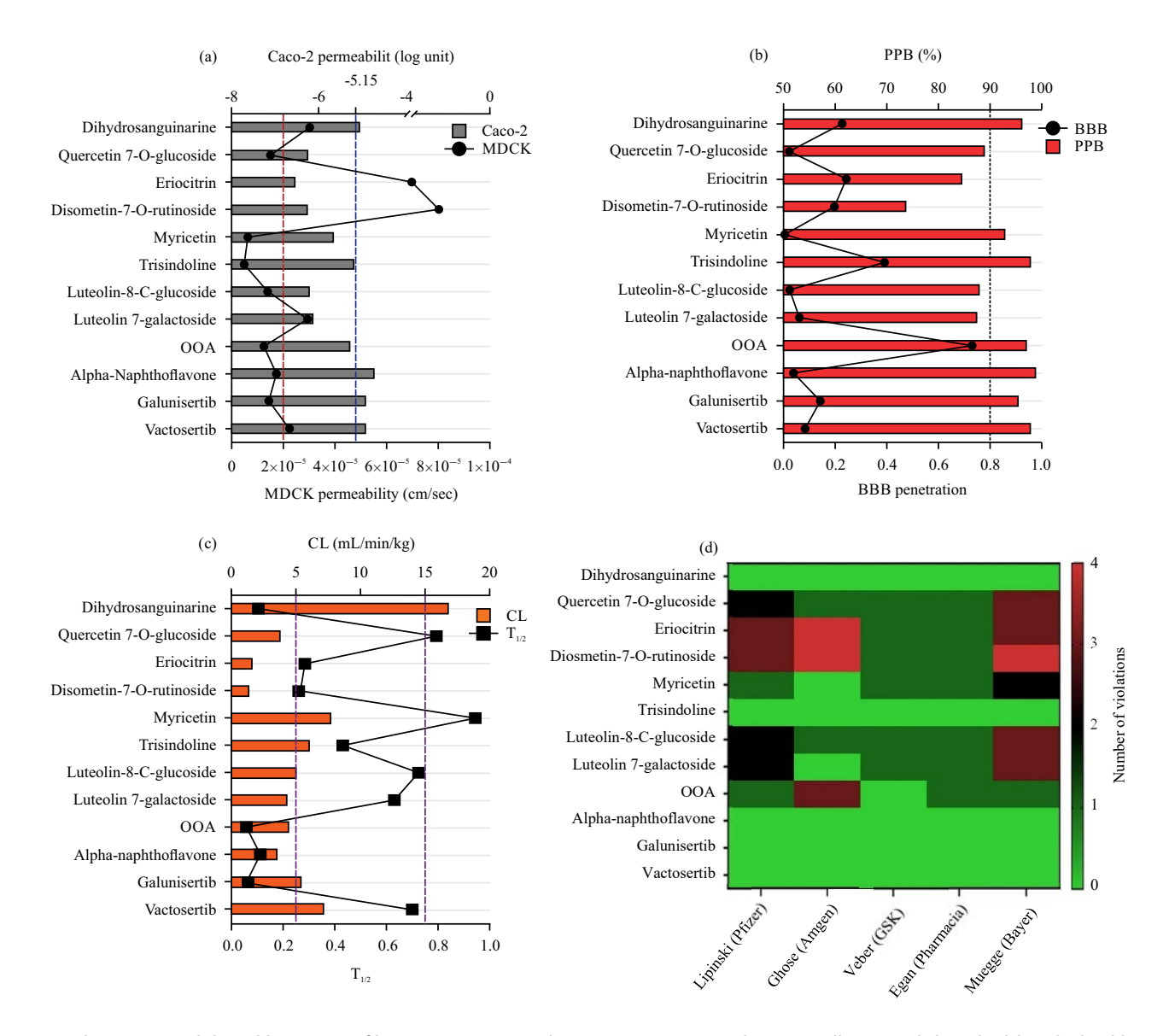


Fig. 8(a-d): ADME and drug-likeness profiles estimation, (a) Absorption: Caco-2 and MDCK cell permeability; the blue dashed line defines the lower limit for Caco-2 permeability, whereas the red dotted line margins the upper limit of MDCK permeability, (b) Distribution: The black dashed line defines the upper limit of PPB, whereas the score of BBB is interpreted as: 0-0.3: Excellent; 0.3-0.7: Medium; 0.7-1.0: Poor, (c) Excretion: The purple dashed lines indicate the moderate clearance range; however, the half-life time $(T_{1/2})$ is estimated at \leq 3 hrs if the score is 0 and >3 hrs at the score of 1 and (d) Heatmap of the drug-likeness rule filters

The MMP2 (gelatinase A) and MMP13 (collagenase 3) are matrix metalloproteinase enzymes. These enzymes are vital in tissue remodeling, wound healing and extracellular matrix (ECM) degradation. They are involved in the pathogenesis of liver cirrhosis. Under normal conditions, ECM homeostasis is maintained by MMPs and the Tissue Inhibitors of Metalloproteinases (TIMPs). Even though that MMPs have inhibitory functions in early stages of liver fibrosis but excessive and prolonged activity may promote the

progression of cirrhosis by allowing the invasion of inflammatory cells and promoting angiogenesis^{55,56}. Moreover, higher serum levels of MMP2 and MMP13 is a characteristic diagnostic features of ALC^{57,58}. The understanding of MMP2 and MMP13 in liver cirrhosis is still an active area of research and therapeutic targeting of these enzymes may hold promise in the development of novel treatment strategies for liver cirrhosis. However, it's important to keep in mind that the liver is a complex organ with multiple interacting pathways and

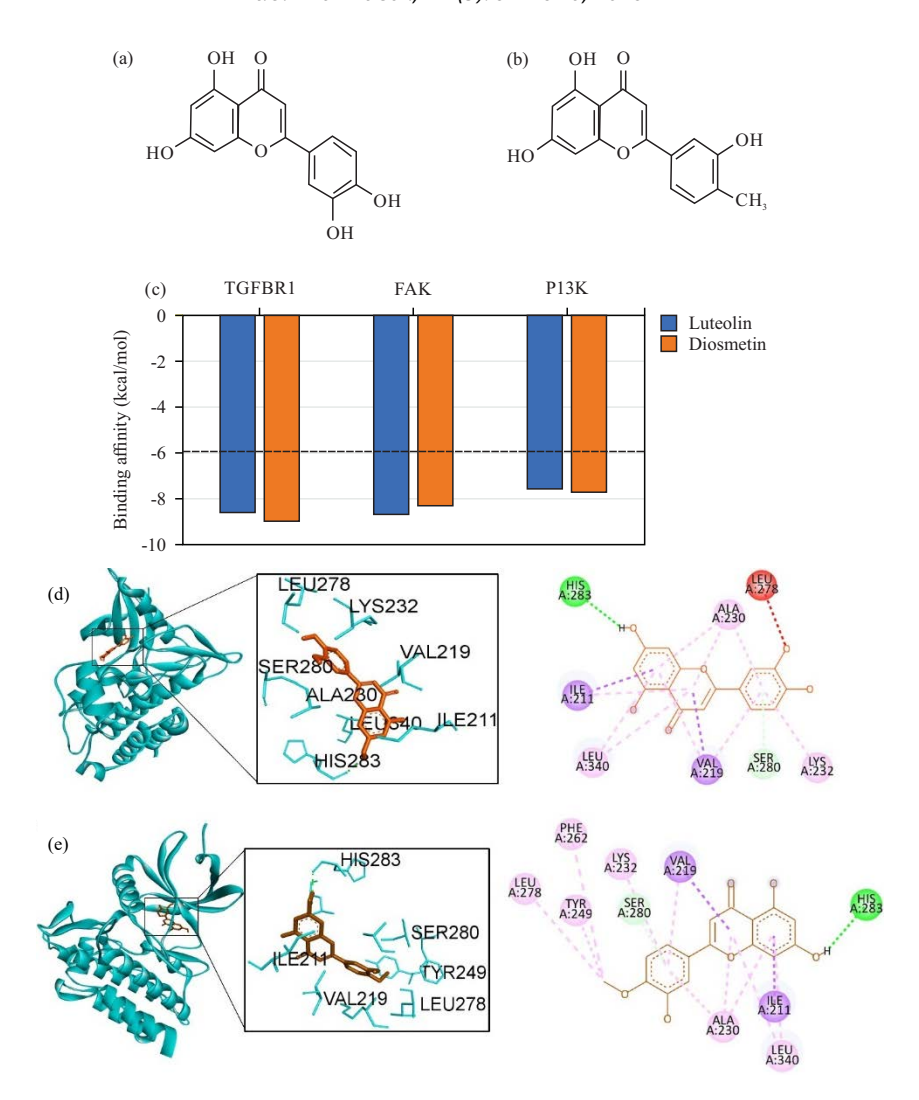


Fig. 9(a-e): Molecular docking analysis of experimentally validated compounds, (a) 2D chemical structure of Luteolin, (b) 2D chemical structure of Diosmetin, (c) Docking scores of Luteolin and Diosmetin with TGFBR1, illustrating their relative binding affinities and potential inhibitory strength, (d) 3D visualization of the co-crystallized structure of TGFBR1 with Luteolin, highlighting the binding pocket and specific interacting amino acid residues and (e) Structural representation of TGFBR1 complexed with Diosmetin, showing detailed interactions and residues contributing to liqand stabilization within the active site

cirrhosis is a multifactorial disease with various etiologies. Therefore, the role of MMP2 and MMP13 in liver cirrhosis may vary depending on the specific etiology and stage of the disease. Current bioinformatics findings revealed the prediction of MMP2 and MMP13 as potential targets for the selected KCB hit compounds. Furthermore, MD results showed off lower affinity scores than the threshold score (-6.0 kcal/mol), indicating the good binding interactions with MMP13 (Table S4).

Dihydrosanguinarine (DHS) is a derivative of the alkaloid sanguinarine, which is found in various plant species, including Papaveraceae. Sanguinarine and its derivatives have been of interest to researchers due to their potential

biological activities, including antimicrobial, anticancer, anti-inflammatory and antioxidant properties^{59,60}. Among the best selected hit compounds, DHS had the lowest binding affinities to TGFβR1 and FAK. However, eriocitrin had the best affinity to Pl3K and MMP13 (Fig. 2 and Table S3). Eriocitrin (Eriodictyol 7-O-rutinoside) is a flavonoid glycoside found in various plants, particularly in the peels of citrus fruits such as lemons, oranges and grapefruits. It is a derivative of the flavonoid eriodictyol and is known for its potential health benefits due to its antioxidant and anti-inflammatory properties⁶¹. According to the aforementioned, both DHS and eriocitrin could be novel therapeutic candidates with antifibrogenic effects against LC.

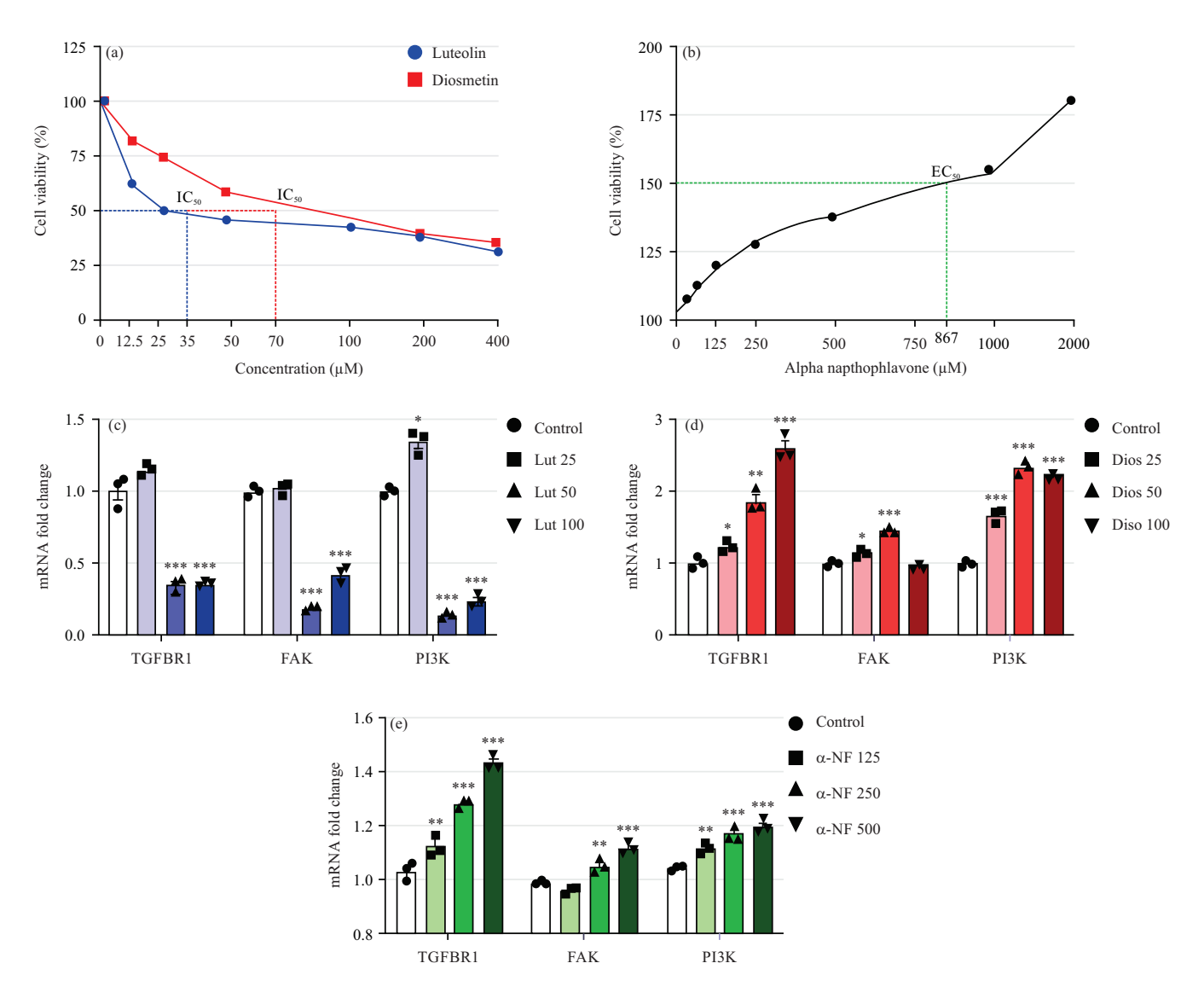


Fig. 10(a-e): *In vitro* experimental validation of flavonoids' effects, (a-b) Cell viability of HepG2 cells and (c-e) Relative mRNA expression

(a-b) Graphs showing the impact of flavonoid treatments-Luteolin, Diosmetin and α -NF-on the viability of HepG2 liver cancer cells after 48 hrs of exposure. Statistically significant differences compared to the untreated control group (0) are denoted by symbols (*p<0.05, **p<0.01 and ***p<0.001), analyzed using a two-tailed unpaired t-test and (c-e) Bar graphs representing changes in mRNA expression levels of target proteins in HepG2 cells treated with the flavonoids for 48 hrs. Statistical differences from the control group are marked (*p<0.05, **p<0.01 and ***p<0.001), assessed via one-way ANOVA

The liver plays a central role in drug metabolism and elimination and in cirrhosis, these processes are significantly altered. The reduced hepatic blood flow, decreased functional liver tissue and altered enzyme activity compromise drug metabolism, leading to prolonged drug half-lives and potential drug accumulation. Additionally, the disrupted bile excretion impairs drug absorption into the intestines, further contributing to altered pharmacokinetics 62 . Typically, any drug candidate should have a long half-life time ($T_{1/2}$) to allow for dosage reduction and thus minimal toxic

effects⁶³. Accordingly, the ADME and drug-likeness profiles demonstrated that DHS, trisindoline, OOA and α -NF could be acceptable drug candidates for LC as they exhibited excellent oral bioavailability results (Fig. 8).

According to Molinspiration bioactivity scores, the investigated small molecules could be classified as active (> 0), moderately active (-0.5 to 0) and inactive (<-0.5) 64 . Therefore and since targeted multi-kinase receptors of LC, the prediction results exhibited a total of seven compounds as active kinase inhibitors (Table 1).

The binding interaction between a ligand and a target protein can lead to either activation or inhibition of the receptor. The in vitro results suggested that luteolin had inhibitory effects on the target proteins, leading to cell death. However, the activatory effects of diosmetin and α -NF on the target proteins represented that TGF-BR1 could play dual roles in apoptosis and cell survival leading to HCC progression (Fig. 10). Moreover, it has been reported that luteolin and diosmetin had anticancer effects on HepG2 cells IC₅₀ values of 9 μ g/mL (31.4 μ M) and 12 μ g/mL (39 μ M), respectively targeting TGF-β signaling pathway^{65,66}. Furthermore, Xia et al.⁶⁷ reported hepatoprotective effects of α -NF against both in vitro and in vivo models of Non-Alcoholic Fatty Liver Disease (NAFLD)⁶⁷. These findings were partially correlated with current in vitro analysis results (Fig. 10), which supported the anticancer effects of both luteolin and diosmetin and also suggested the potential protective effects of α -NF against chronic liver disease models.

CONCLUSION

This study has conducted a virtual screening of the KCB natural compounds library with multiple kinases related to LC pathogenesis. Using MD, promising multi-kinase ligands were identified targeting the non-canonical TGF-β signaling pathway. However, through bioinformatics, an essential enzyme receptor, MMP13, was predicted as a potential target by the hit compounds. Moreover, the predicted ADMET profile results exhibited three compounds (DHS, trisindoline and α -NF) that ideally fit the standard drug-likeness parameters as oral drug candidates. However, strongly recommended to conduct further preclinical studies to investigate the potential effects of these natural compounds, particularly DHS, trisindoline and α -NF on *in vitro* and *in vivo* models of chronic liver injury for more validation and confirmation of the docking findings and the efficacy of the targeted mechanism of action.

SIGNIFICANCE STATEMENT

Liver cirrhosis is a major global health burden driven by TGF-β-mediated fibrosis. This study employed molecular docking and bioinformatics to screen the Korea Chemical Bank (KCB) natural compounds library, identifying multi-target inhibitors for TGF-βR1, FAK and PI3K. Promising candidates, including dihydrosanguinarine (DHS) and eriocitrin, showed high binding affinities, while ADMET analysis confirmed their oral bioavailability and drug-likeness. The RT-qPCR validation revealed luteolin's inhibitory effects on fibrogenic genes,

suggesting its therapeutic relevance. These findings highlight the potential of natural compounds for antifibrotic therapy. Future studies should focus on *in vivo* validation, mechanistic analyses and drug formulation to optimize their therapeutic efficacy and clinical applicability for liver cirrhosis treatment. This research expands current knowledge on multi-target natural drug discovery for liver cirrhosis.

ACKNOWLEDGMENT

Special acknowledgments to Korea Research Institute of Chemical Technology (KRICT) and KCB for providing PDB files of the natural product library. Also, our acknowledge all contributors to *in silico* techniques used in this study, particularly the web designers and software developers. The Basic Science Research Program of the National Research Foundation of Korea (NRF), funded by the Ministry of Science, ICT and Future Planning, supported this study with grants No. 2021R1A2C1004184 (to H-J.C.) No. 2021R1A2C1004133 (to N.Y.J.) and No. 2023R1A2C1003763 (to J.J.).

REFERENCES

- 1. Schuppan, D. and N.H. Afdhal, 2008. Liver cirrhosis. Lancet, 371: 838-851.
- 2. Dooley, S. and P. ten Dijke, 2012. TGF-β in progression of liver disease. Cell Tissue Res., 347: 245-256.
- 3. Dewidar, B., J. Soukupova, I. Fabregat and S. Dooley, 2015. TGF-β in hepatic stellate cell activation and liver fibrogenesis: updated. Curr. Pathobiol. Rep., 3: 291-305.
- Shi, X., C.D. Young, H. Zhou and X.J. Wang, 2020. Transforming growth factor-β signaling in fibrotic diseases and cancer-associated fibroblasts. Biomolecules, Vol. 10. 10.3390/biom10121666.
- Friedman, S.L., 2008. Hepatic stellate cells: Protean, multifunctional, and enigmatic cells of the liver. Physiol. Rev., 88: 125-172.
- 6. Kisseleva, T., 2017. The origin of fibrogenic myofibroblasts in fibrotic liver. Hepatology, 65: 1039-1043.
- 7. Herbertz, S., J.S. Sawyer, A.J. Stauber, I. Gueorguieva and K.E. Driscoll *et al.*, 2015. Clinical development of galunisertib (LY2157299 monohydrate), a small molecule inhibitor of transforming growth factor-beta signaling pathway. Drug Des. Dev. Ther., 9: 4479-4499.
- 8. Lee, H.J., 2020. Recent advances in the development of TGF- β signaling inhibitors for anticancer therapy. J. Cancer Prev., 25: 213-222.
- Kitchen, D.B., H. Decornez, J.R. Furr and J. Bajorath, 2004.
 Docking and scoring in virtual screening for drug discovery:
 Methods and applications. Nat. Rev. Drug Discovery, 3: 935-949.

- Morris, G.M., D.S. Goodsell, R.S. Halliday, R. Huey, W.E. Hart, R.K. Belew and A.J. Olson, 1998. Automated docking using a Lamarckian genetic algorithm and an empirical binding free energy function. J. Comput. Chem., 19: 1639-1662.
- 11. Shoichet, B.K., 2004. Virtual screening of chemical libraries. Nature, 432: 862-865.
- 12. Chen, S.R., X.P. Chen, J.J. Lu, Y. Wang and Y.T. Wang, 2015. Potent natural products and herbal medicines for treating liver fibrosis. Chin. Med., Vol. 10. 10.1186/s13020-015-0036-y.
- 13. Ma, X., Y. Jiang, J. Wen, Y. Zhao, J. Zeng and Y. Guo, 2020. A comprehensive review of natural products to fight liver fibrosis: Alkaloids, terpenoids, glycosides, coumarins and other compounds. Eur. J. Pharmacol., Vol. 888. 10.1016/j.ejphar.2020.173578.
- Temirak, A., M. Abdulla and M. Elhefnawi, 2012. Rational drug design for identifying novel multi-target inhibitors for hepatocellular carcinoma. Anti-Cancer Agents Med. Chem., 12: 1088-1097.
- Zhang, Q., Z. Feng, M. Gao and L. Guo, 2021. Determining novel candidate anti-hepatocellular carcinoma drugs using interaction networks and molecular docking between drug targets and natural compounds of SiNiSan. PeerJ, Vol. 9. 10.7717/peerj.10745.
- Zheng, Y., S. Ji, X. Li and Q. Feng, 2022. Active ingredients and molecular targets of *Taraxacum mongolicum* against hepatocellular carcinoma: Network pharmacology, molecular docking, and molecular dynamics simulation analysis. PeerJ, Vol. 10. 10.7717/peerj.13737.
- Emoniem, N.A, R.M. Mukhtar, H. Ghaboosh, E.M. Elshamly, M.A. Mohamed, T. Elsaman and A.A. Alzain, 2023. Turning down PI3K/AKT/mTOR signalling pathway by natural products: An *in silico* multi-target approach. SAR QSAR Environ. Res., 34: 163-182.
- Morris, G.M., R. Huey, W. Lindstrom, M.F. Sanner, R.K. Belew, D.S. Goodsell and A.J. Olson, 2009. AutoDock4 and AutoDockTools4: Automated docking with selective receptor flexibility. J. Comput. Chem., 30: 2785-2791.
- O'Boyle, N.M., M. Banck, C.A. James, C. Morley, T. Vandermeersch and G.R. Hutchison, 2011. Open Babel: An open chemical toolbox. J. Cheminf., Vol. 3. 10.1186/1758-2946-3-33.
- Eberhardt, J., D. Santos-Martins, A.F. Tillack and S. Forli, 2021.
 AutoDock Vina 1.2.0: New docking methods, expanded force field, and python bindings. J. Chem. Inf. Model., 61: 3891-3898.
- 21. Tebben, A.J., M. Ruzanov, M. Gao, D. Xie and S.E. Kiefer *et al.*, 2016. Crystal structures of apo and inhibitor-bound TGFβR2 kinase domain: Insights into TGFβR isoform selectivity. Acta Crystallogr. Sect. D Struct. Biol., 72: 658-674.
- 22. Roberts, W.G., E. Ung, P. Whalen, B. Cooper and C. Hulford *et al.*, 2008. Antitumor activity and pharmacology of a selective focal adhesion kinase inhibitor, PF-562,271. Cancer Res., 68: 1935-1944.

- 23. Terstiege, I., M. Perry, J. Petersen, C. Tyrchan, T. Svensson, H. Lindmark and L. Öster, 2017. Discovery of triazole aminopyrazines as a highly potent and selective series of PI3Kδ inhibitors. Bioorg. Med. Chem. Lett., 27: 679-687.
- 24. Berman, H.M., J. Westbrook, Z. Feng, G. Gilliland and T.N. Bhat *et al.*, 2000. The protein data bank. Nucleic Acids Res., 28: 235-242.
- Piñero, J., J.M. Ramírez-Anguita, J. Saüch-Pitarch, F. Ronzano, E. Centeno, F. Sanz and L.I. Furlong, 2020. The DisGeNET knowledge platform for disease genomics: 2019 update. Nucleic Acids Res., 48: D845-D855.
- Daina, A., O. Michielin and V. Zoete, 2019. SwissTargetPrediction: Updated data and new features for efficient prediction of protein targets of small molecules. Nucleic Acids Res., 47: W357-W364.
- 27. Sherman, B.T., M. Hao, J. Qiu, X. Jiao and M.W. Baseler *et al.*, 2022. DAVID: A web server for functional enrichment analysis and functional annotation of gene lists (2021 update). Nucleic Acids Res., 50: W216-W221.
- 28. Szklarczyk, D., A. Franceschini, S. Wyder, K. Forslund and D. Heller *et al.*, 2015. STRING v10: Protein-protein interaction networks, integrated over the tree of life. Nucleic Acids Res., 43: D447-D452.
- 29. Shannon, P., A. Markiel, O. Ozier, N.S. Baliga and J.T. Wang *et al.*, 2003. Cytoscape: A software environment for integrated models of biomolecular interaction networks. Genome Res., 13: 2498-2504.
- 30. Xiong, G., Z. Wu, J. Yi, L. Fu and Z. Yang *et al.*, 2021. ADMETlab 2.0: An integrated online platform for accurate and comprehensive predictions of ADMET properties. Nucleic Acids Res., 49: W5-W14.
- Daina, A., O. Michielin and V. Zoete, 2017. SwissADME: A free web tool to evaluate pharmacokinetics, drug-likeness and medicinal chemistry friendliness of small molecules. Sci. Rep., Vol. 7. 10.1038/srep42717.
- 32. Park, K.H., H.M.M. Makki, S.H. Kim, H.J. Chung and J. Jung, 2023. Narirutin ameliorates alcohol-induced liver injury by targeting MAPK14 in zebrafish larvae. Biomed. Pharmacother., Vol. 166. 10.1016/j.biopha.2023.115350.
- 33. Trott, O. and A.J. Olson, 2010. AutoDock vina: Improving the speed and accuracy of docking with a new scoring function, efficient optimization, and multithreading. J. Comput. Chem., 31: 455-461.
- Ramírez, D. and J. Caballero, 2018. Is it reliable to take the molecular docking top scoring position as the best solution without considering available structural data? Molecules, Vol. 23. 10.3390/molecules23051038.
- 35. de Savi, C., A.D. Morley, I. Nash, G. Karoutchi, K. Page, A. Ting and S. Gerhardt, 2012. Lead optimisation of selective non-zinc binding inhibitors of MMP13. Part 2. Bioorg. Med. Chem. Lett., 22: 271-277.

- 36. Lipinski, C.A., F. Lombardo, B.W. Dominy and P.J. Feeney, 2001. Experimental and computational approaches to estimate solubility and permeability in drug discovery and development settings. Adv. Drug Delivery Rev., 46: 3-26.
- 37. Ghose, A.K., V.N. Viswanadhan and J.J. Wendoloski, 1999. A knowledge-based approach in designing combinatorial or medicinal chemistry libraries for drug discovery. 1. A qualitative and quantitative characterization of known drug databases. J. Comb. Chem., 113: 55-68.
- 38. Veber, D.F., S.R. Johnson, H.Y. Cheng, B.R. Smith, K.W. Ward and K.D. Kopple, 2002. Molecular properties that influence the oral bioavailability of drug candidates. J. Med. Chem., 45: 2615-2623.
- 39. Egan, W.J., K.M. Merz and J.J. Baldwin, 2000. Prediction of drug absorption using multivariate statistics. J. Med. Chem., 43: 3867-3877.
- 40. Muegge, I., S.L. Heald and D. Brittelli, 2001. Simple selection criteria for drug-like chemical matter. J. Med. Chem., 44: 1841-1846.
- 41. Pinter, M., M. Trauner, M. Peck-Radosavljevic and W. Sieghart, 2016. Cancer and liver cirrhosis: Implications on prognosis and management. ESMO Open, Vol. 1. 10.1136/esmoopen-2016-000042.
- 42. D'Amico, G., G. Garcia-Tsao and L. Pagliaro, 2006. Natural history and prognostic indicators of survival in cirrhosis: A systematic review of 118 studies. J. Hepatol., 44: 217-231.
- 43. Weiskirchen, R. and F. Tacke, 2016. Liver fibrosis: From pathogenesis to novel therapies. Digestive Dis., 34: 410-422.
- 44. Marcellin, P., E. Gane, M. Buti, N. Afdhal and W. Sievert *et al.*, 2013. Regression of cirrhosis during treatment with tenofovir disoproxil fumarate for chronic hepatitis B: A 5-year open-label follow-up study. Lancet, 381: 468-475.
- 45. Schuppan, D., M. Ashfaq-Khan, A.T. Yang and Y.O. Kim, 2018. Liver fibrosis: Direct antifibrotic agents and targeted therapies. Matrix Biol., 68-69: 435-451.
- 46. Meli, R., G.M. Morris and P.C. Biggin, 2022. Scoring functions for protein-ligand binding affinity prediction using structure-based deep learning: A review. Front. Bioinf., Vol. 2. 10.3389/fbinf.2022.885983.
- 47. Nusantoro, Y.R. and A. Fadlan, 2021. The effect of energy minimization on the molecular docking of acetone-based oxindole derivatives. Jurnal Kimia dan Pendidikan Kimia, 6: 69-77.
- 48. Shityakov, S. and C. Foerster, 2014. *In silico* predictive model to determine vector-mediated transport properties for the blood-brain barrier choline transporter. Adv. Appl. Bioinf. Chem., 7: 23-36.
- 49. Molagoda, I.M.N., S.S. Sanjaya, K.T. Lee, Y.H. Choi and J.H. Lee *et al.*, 2023. Derrone targeting the TGF type 1 receptor kinase improves bleomycin-mediated pulmonary fibrosis through inhibition of Smad signaling pathway. Int. J. Mol. Sci., Vol. 24. 10.3390/ijms24087265.

- 50. Xia, H., R.S. Nho, J. Kahm, J. Kleidon and C.A. Henke, 2004. Focal adhesion kinase is upstream of phosphatidylinositol 3-kinase/Akt in regulating fibroblast survival in response to contraction of type I collagen matrices via a β_1 integrin viability signaling pathway. J. Biol. Chem., 279: 33024-33034.
- 51. Park, S.A., M.J. Kim, S.Y. Park, J.S. Kim, W. Lim, J.S. Nam and Y.Y. Sheen, 2015. TIMP-1 mediates TGF-β-dependent crosstalk between hepatic stellate and cancer cells via FAK signaling. Sci. Rep., Vol. 5. 10.1038/srep16492.
- 52. Molla, M.H.R., M.O. Aljahdali, M.A.A. Sumon, A.H. Asseri, H.N. Altayb *et al.*, 2023. Integrative ligand-based pharmacophore modeling, virtual screening, and molecular docking simulation approaches identified potential lead compounds against pancreatic cancer by targeting FAK1. Pharmaceuticals, Vol. 16. 10.3390/ph16010120.
- 53. Wu, F., T. Xu, G. He, L. Ouyang and B. Han *et al.*, 2012. Discovery of novel focal adhesion kinase inhibitors using a hybrid protocol of virtual screening approach based on multicomplex-based pharmacophore and molecular docking. Int. J. Mol. Sci., 13: 15668-15678.
- Al Hasan, M., M. Sabirianov, G. Redwine, K. Goettsch, S.X. Yang and H.A. Zhong, 2023. Binding and selectivity studies of phosphatidylinositol 3-kinase (PI3K) inhibitors. J. Mol. Graphics Modell., Vol. 121. 10.1016/j.jmgm.2023.108433.
- 55. Parks, W.C., C.L. Wilson and Y.S. López-Boado, 2004. Matrix metalloproteinases as modulators of inflammation and innate immunity. Nat. Rev. Immunol., 4: 617-629.
- 56. Giannandrea, M. and W.C. Parks, 2014. Diverse functions of matrix metalloproteinases during fibrosis. Dis. Models Mech., 7: 193-203.
- 57. Prystupa, A., M. Szpetnar, A. Boguszewska-Czubara, A. Grzybowski, J. Sak, W. Załuska, 2015. Activity of MMP1 and MMP13 and amino acid metabolism in patients with alcoholic liver cirrhosis. Med. Sci. Monit., 21: 1008-1014.
- 58. Roeb, E., 2018. Matrix metalloproteinases and liver fibrosis (translational aspects). Matrix Biol., 68-69: 463-473.
- 59. Wu, S.Z., H.C. Xu, X.L. Wu, P. Liu and Y.C. Shi *et al.*, 2019. Dihydrosanguinarine suppresses pancreatic cancer cells via regulation of mut-p53/WT-p53 and the Ras/Raf/Mek/Erk pathway. Phytomedicine, Vol. 59. 10.1016/j.phymed.2019.152895.
- 60. Xiang, Y., H. Zhang, Z.X. Zhang, X.Y. Qu and F.X. Zhu, 2022. Dihydrosanguinarine based RNA-seq approach couple with network pharmacology attenuates LPS-induced inflammation through TNF/IL-17/PI3K/AKT pathways in mice liver. Int. Immunopharmacol., Vol. 109. 10.1016/j.intimp.2022.108779.
- 61. Yao, L., W. Liu, M. Bashir, M.F. Nisar and C.C. Wan, 2022. Eriocitrin: A review of pharmacological effects. Biomed. Pharmacother., Vol. 154. 10.1016/j.biopha.2022.113563.

- 62. Weersink, R.A., D.M. Burger, K.L. Hayward, K. Taxis, J.P.H. Drenth and S.D. Borgsteede, 2020. Safe use of medication in patients with cirrhosis: pharmacokinetic and pharmacodynamic considerations. Expert Opin. Drug Metab. Toxicol., 16: 45-57.
- 63. Dulsat, J., B. López-Nieto, R. Estrada-Tejedor and J.I. Borrell, 2023. Evaluation of free online ADMET tools for academic or small biotech environments. Molecules, Vol. 28. 10.3390/molecules28020776.
- 64. Mijanur Rahman, A. Talukder and R. Akter, 2021. Computational designing and prediction of ADMET properties of four novel imidazole-based drug candidates inhibiting heme oxygenase-1 causing cancers. Mol. Inf., Vol. 40. 10.1002/minf.202060033.
- 65. Yee, S.B., H.J. Choi, S.W. Chung, D.H. Park, B. Sung, H.Y. Chung and N.D. Kim, 2015. Growth inhibition of luteolin on HepG2 cells is induced via p53 and Fas/Fas-ligand besides the TGF-β pathway. Int. J. Oncol., 47: 747-754.
- 66. Liu, B., Y. Shi, W. Peng, Q. Zhang, J. Liu, N. Chen and R. Zhu, 2016. Diosmetin induces apoptosis by upregulating p53 via the TGF-β signal pathway in HepG2 hepatoma cells. Mol. Med. Rep., 14: 159-164.
- 67. Xia, H., X. Zhu, X. Zhang, H. Jiang and B. Li *et al.*, 2019. Alpha-naphthoflavone attenuates non-alcoholic fatty liver disease in oleic acid-treated HepG2 hepatocytes and in high fat diet-fed mice. Biomed. Pharmacother., Vol. 118. 10.1016/j.biopha.2019.109287.

SUPPLEMENTARY MATERIALS

Table S1: PDB codes of target receptors

Macromolecule (Receptor)	PDB accession code
Transforming Growth Factor Receptor Type 1 (TGFBR1)	5E8S
Focal Adhesion Kinase (FAK)	3BZ3
Phosphoinositide 3-Kinase (PI3K)	5T23
Matrix Metallopeptidase 13 (MMP13)	4A7B

Table S2: Primer list and sequences

Name	Forward (5'-3')	Reverse (5'-3')
TGFBR1	GACAACGTCAGGTTCTGGCTCA	CCGCCACTTTCCTCCAAACT
FAK (PTK2)	GCCTTATGACGAAATGCTGGGC	CCTGTCTTCTGGACTCCATCCT
PIK3CA	GAAGCACCTGAATAGGCAAGTCG	GAGCATCCATGAAATCTGGTCGC
GAPDH	GTCTCCTCTGACTTCAACAGCG	ACCACCCTGTTGCTGTAGCCAA

Table S3: SMILES structures and docking scores of the best 10 TGFBR1 inhibitors

				Binding at	ffinity (kcal/mol)	
Compound No.	. Small molecule (Ligand)	SMILES structure	PubChem CID	TGFBR1	FAK	PI3K
1252	Dihydrosanguinarine	CN1CC2=C3OCOC3=CC=C2C4=C1C5=C(C=C4)C=C6OCOC6=C5	124069	-11.2	-10.1	-9.1
125	Quercetin 7-O-glucoside	OCC1OC(OC2=CC3=C(C(=C2)O)C(=O)C(=C(O3)C4=CC(=C(O)	5381351	-11.1	-8.9	-9.8
		C=C4)O)O)C(O)C(O)C1O				
225	Eriocitrin	CC1OC(OCC2OC(OC3=CC(=C4C(=O)CC(OC4=C3)C5=CC=C(O)	3564542	-10.9	-9.5	-10.5
		C(=C5)O)O)C(O)C(O)C(O)C(O)C(O)C1O				
298	Diosmetin-7-O-rutinoside	COC1=C(0)C=C(C=C1)C2=CC(=0)C3=C(0)C=C(0C40C(COC50C	5353588	-10.9	-9.0	-9.9
		(C)C(O)C(O)C5O)C(O)C(O)C4O)C=C3O2				
90	Myricetin	OC1=CC(=C2C(=O)C(=C(OC2=C1)C3=CC(=C(O)C(=C3)O)O)O)O	5281672	-10.7	-8.6	-9.0
119	Trisindoline	O=C1NC2=C(C=CC=C2)C1(C3=C[NH]C4=CC=CC=C34)	2883607	-10.6	-9.7	-8.6
		C5=C[NH]C6=C5C=CC=C6				
304	Luteolin-8-C-glucoside	OCC1OC(C(0)C(0)C10)C2=C3OC(=CC(=0)C3=C(0)	5382105	-10.5	-8.4	-8.4
		C=C2O)C4=CC(=C(O)C=C4)O				
33	Luteolin 7-galactoside	OCC1OC(OC2=CC3=C(C(=C2)O)C(=O)C=C(O3)	5291488	-10.4	-9.1	-9.5
		C4=CC=C(O)C(=C4)O)C(O)C(O)C1O				
164	3-Oxolup-20(29)-en-28-oic acid	CC(=C)C1CCC2(CCC3(C)C(CCC4C5(C)CCC(=O)	289985	-10.4	-8.1	-6.8
		C(C)(C)C5CCC34C)C12)C(O)=O				
438	Alpha-naphthoflavone	O=C1C=C(OC2=C1C=CC3=CC=CC23)C4=CC=CC4	11790	-10.4	-9.3	-10.1
-	Galunisertib	CC1=CC=CC(=N1)C2=NN3CCCC3=C2C4=C5C=C	10090485	-10	-10.7	-9.4
		(C=CC5=NC=C4)C(N)=O				
-	Vactosertib	CC1=CC=CC(=N1)C2=C(N=C(CNC3=CC=CC=C3F)N2)	54766013	-10.6	-9.7	-9.3
		C4=CN5N=CN=C5C=C4				

Int. J. Pharmacol., 21 (3): 521-540, 2025

Table S4: Docking scores with MMP13

		Binding affinity (kcal/mol)		
Compound No.	Small molecule (Ligand)	Chain A	Chain B	
1252	Dihydrosanguinarine	-8.3	-7.6	
125	Quercetin 7-O-glucoside	-8.7	-9.1	
225	Eriocitrin	-9.5	-9.8	
298	Diosmetin-7-O-rutinoside	-8.9	-9.1	
90	Myricetin	-8.9	-8.7	
119	Trisindoline	-6.1	-9.0	
304	Luteolin-8-C-glucoside	-7.2	-8.5	
33	Luteolin 7-galactoside	-9.3	-9.3	
164	3-Oxolup-20(29)-en-28-oic acid	-5.8	-7.0	
438	alpha-Naphthoflavone	-9.3	-9.7	
-	Galunisertib	-8.8	-9.0	
-	Vactosertib	-9.6	-9.7	